Treatment Planning of Carbon-Ion Radiotherapy

Nobuyuki Kanematsu and Taku Inaniwa

Abstract

Treatment planning of carbon-ion radiotherapy (C-ion RT) should best use the physical and biological advantages of the radiation, which is heavily coupled to the beam delivery system. In this section, overview of conventional system for broad-beam delivery, which has been used for many years, and a state-of-the-art system for pencil-beam scanning are described in addition to general aspects to plan a treatment of carbon-ion radiotherapy. Finally, we demonstrate the comparison between broad- and scanning-beam plans for a few cases.

Keywords

Broad beam • Dose calculation • Plan optimization • Scanning beam

11.1 Introduction

Treatment planning is a process to design radiation beams to achieve the optimum balance between dose conformation to a target and sparing of normal tissues and to evaluate the resultant dose to the patient. In this regard, treatment planning of C-ion RT is not at all different from treatment planning of other radiotherapy modalities. There are of course intrinsically distinctive features in carbon-ion radiotherapy, which must be best used for cancer treatment.

11.1.1 Physical Properties of Carbon Ions

Carbon ion and proton are heavy charged particles that are currently used for radiotherapy. A most favorable feature of these particles is formation of a Bragg peak dose at a certain depth of penetration, which can be placed to a tumor by adjusting the incident energy. A fully stripped carbon ion (or atomic nucleus) is a composite of six protons and six neutrons. Compared to a proton, its electric charge is a factor of 6 larger and its mass is approximately a factor of 12 larger. This makes differences to radiological properties between carbon-ion and proton beams:

- A carbon ion has 36 times higher LET for the same speed and 12 times more kinetic energy, resulting in reduced range to 1/3.
- Higher speed is thus required to achieve the same range, which makes carbon ion more rigid in addition to halved charge/mass ratio, resulting in reduced scattering to 28 % for the same range.
- Due to its larger size, loss of carbon ions by nuclear interactions is a few times larger than that of protons. About a half of carbon ions may be lost in 20 cm of penetration in water.
- The nuclear interactions may cause fragmentation of the nucleus into lighter nuclei, resulting unwanted fragmentation tail after the Bragg peak.

The reduced scattering, namely, sharper penumbra, is usually an advantage in radiation therapy, while increased nuclear interactions, namely, reduced Bragg peak, are clearly a disadvantage.

N. Kanematsu (✉) • T. Inaniwa
National Institute of Radiological Sciences, 9-1, Anagawa-4, Inage-ku, Chiba 263-8555, Japan
e-mail: nkanemat@nirs.go.jp; taku@nirs.go.jp

11.1.2 Radiobiological Modeling

In radiation biology, relative biological effectiveness (RBE) is defined as the ratio of a reference-radiation dose to an interest-radiation dose for the same biological endpoint under the same condition other than the radiation quality. For therapeutic applications, the RBE naturally depends on fraction dose size and clinical endpoint, which vary with tumor type, tumor site, and treatment intent. In addition, as the radiation quality of a carbon-ion beam varies with incident energy, range modulation, and penetration depth, the RBE varies in patient body within each single beam. Generally the RBE increases with depth in the spread-out Bragg peak (SOBP) region.

Because all these complex dependences of the RBE have not been accurately known, the RBE used in treatment planning (clinical RBE) may be only considered as assumption rather than estimation. Unlike estimation, to which uncertainty must always be associated, an unambiguously defined clinical RBE is used for the RBE-weighted absorbed dose to water to evaluate the clinically relevant dose. Unless otherwise specified, "dose" in treatment planning of C-ion RT refers to the RBE-weighted absorbed dose to water.

For photon beams, for example, absorbed dose to water in units of Gy is used for prescription although there is always variation in responsiveness of the tumor to the dose, which may vary significantly due to unknown or uncontrollable factors in clinical environment. In other words, the photon beam dose, against which the RBE is normally referenced, has intrinsic limitation for clinical relevance. It would be therefore a reasonable approach to consider the clinical dose as proper to carbon-ion beams and optimize its prescription in clinical studies systematically without relating to photon experiences. From a practical point of view, the precision of prescribed dose should be controlled within a few percent for clinical studies.

An important requirement for the clinical RBE is clarity in definition. NIRS chose to use 10 % cell survival of human salivary gland cells as the biological endpoint with rescaling for continuation of fast-neutron radiotherapy experiences. This clinical RBE has been mathematically defined and in fact has been used consistently in the NIRS, Hyogo Ion Beam Medical Center, and Gunma University for uniform dose prescription among these institutions. The clinical dose is the only quantity that the radiation oncologist may need to evaluate to treat patients with carbon ions while the complexity originated from radiation biology is normally hidden in the treatment planning system.

11.2 General Aspects of Treatment Planning for Carbon-Ion Radiotherapy

11.2.1 Patient Position and Beam Direction

Arrangement of beams is one of the most critical decisions in treatment planning. In the common practice of C-ion RT with fixed beam lines, the beam directions are severely limited. Consequently, multiple patient positions, typically supine and prone, are required for treatment of a tumor. In fact, treatment couches with large rolling capability, typically up to 20°, have been also used in the HIMAC treatment rooms. While a treatment with multiple patient positions and multiple patient rolls may be a reasonable approach to substitute for a rotating gantry, it substantially complicates the treatment process with multiple plans.

11.2.2 Immobilization and Planning CT

Volumetric X-ray computed tomography (CT) image of a patient is the basis of computerized treatment planning. For the planning CT, the patient must be immobilized exactly in the treatment condition. Figure 11.1 demonstrates a scene of planning CT, where a patient was immobilized in tilted position and the scanning timing was synchronized to breathing using the same respiratory gating system used for treatment beam delivery.

11.2.3 ROI Delineation

Anatomical determination of target volumes and organs at risk is a critical oncologic task and the resultant regions of interest (ROI) are used to design and evaluate a plan. Because contrast agents cannot be used for planning CT to secure correct interpretation of the CT number, ROI delineation is often difficult. Contrast-enhanced X-ray CT and magnetic resonance imaging (MRI) may give high-contrast image of patient anatomy. Positron emission tomography (PET) gives metabolic image of tumor as shown in clinical examples in this book. These imaging modalities are thus useful for identification of gross tumor volume (GTV) on the planning CT image, for which advancement of image-processing technologies has enabled computerized image registration and fused display even in the presence of body deformation.

Fig. 11.1 Scene of planning CT for a patient in rolled treatment position with optical respiratory gating
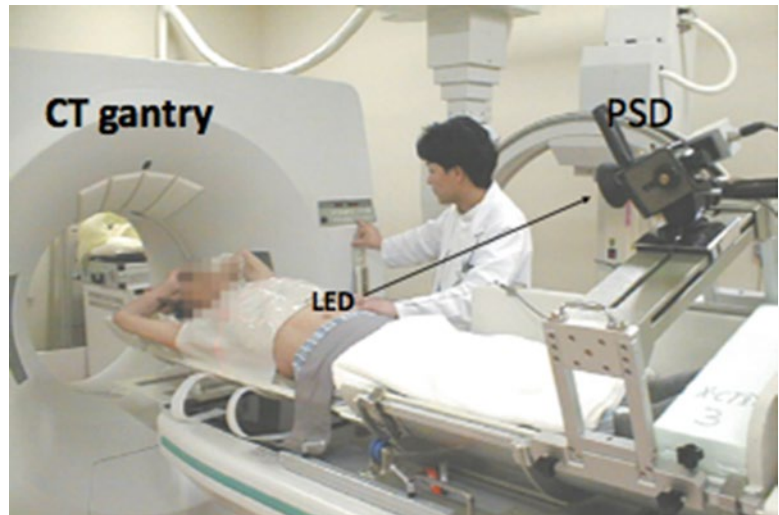
To plan a beam for a tumor, a radiation oncologist first defines a clinical target volume (CTV) that includes the GTV and surrounding region of clinical margin for potential infiltration. The CTV is the volume to be treated in the planning CT. However, there are always differences between planning CT and treatment times due to physiological changes, organ motion, patient setup error, beam model error, etc. All these uncertainties must be considered at the time of planning. To treat the CTV with prescribed dose in reality, appropriate margins need to be added for a planning target volume (PTV), which is intended to receive the prescribed tumor dose in treatment planning. However, it is generally difficult to quantify these uncertainties. In the cases where the dominant uncertainties are expected in the clinical margins, the setup and internal margins may be disregarded. In such cases, the PTV may be defined as identical to the CTV.

Ideally, the margin against all uncertainties should be included in the PTV. Margin for setup error should expand the PTV in lateral direction while that for range error should expand the PTV in depth direction for each field. However, in common practice, the PTV is defined before the beams are set up, which makes it difficult to define field-specific PTV. Therefore, a common practice is to assign only minimum isotropic margin for PTV to account for the setup uncertainty, which is usually smaller than the range uncertainty. Therefore, the excess of the range uncertainty is usually considered by additional depth margin to cover the PTV with an SOBP of each beam.

11.2.4 Patient Modeling

As water is the reference material in radiation dosimetry, patients are modeled volumetrically as water of variable effective density (ED) to design beams and to calculate dose distributions. Precise beam-range control to cover the tumor site with SOBP is the essence of C-ion RT. For this purpose, the ED is defined by the stopping-power ratio of the tissue to water for carbon ions. In the planning CT, the CT number ideally represents the X-ray attenuation ratio of the body tissue to water. The conversion from CT number to ED is based on strong systematic correlation between X-ray attenuation and carbon-ion stopping power for human tissues as shown in Fig. 11.2. The CT-ED relation depends on tube voltage, X-ray filter, and hardening effects. Therefore, precise calibration of the conversion curve is necessary for each CT-scanning condition. The hardening effect is object-dependent and therefore considered to be dominant uncertainty for the conversion based on measurement with calibration phantom. Because the conversion uncertainty is generally assumed to be of the order of 1 %, the precision of conversion curves in the same calibration condition should naturally be below 1 %. As there are no available tissue-equivalent materials that are valid for carbon-ion beams, the construction of the CT-ED relationship requires knowledge of the X-ray energy spectrum and elemental composition of tissues, with which X-ray attenuation coefficient or CT number and stopping-power ratio or ED of body tissues can be associated.

In addition to energy loss of carbon ions, which is the major source of radiation dose, multiple Coulomb scattering and nuclear interactions also influence the dose distribution. The majority of body tissues are nearly equivalent to water, which is abundant in oxygen, while bone tissues are abundant in calcium and adipose tissues are abundant in carbon. These compositional differences are ignored in the ED-based patient model. Generally, this approximation may cause only marginal effects to dose distributions in clinical cases.

Fig. 11.2 Radiological properties of the body tissues in an example stoichiometric calibration; (**a**) and (**c**) are the correlation between linear attenuation coefficient ratio μ and relative electron density ρ_e, (**b**) and (**d**) correlation between μ and stopping-power ratio ρ_S and (**e**) and (**f**) residual histograms of ρ_e and ρ_S, respectively, with respect to the fitting polylines [1]
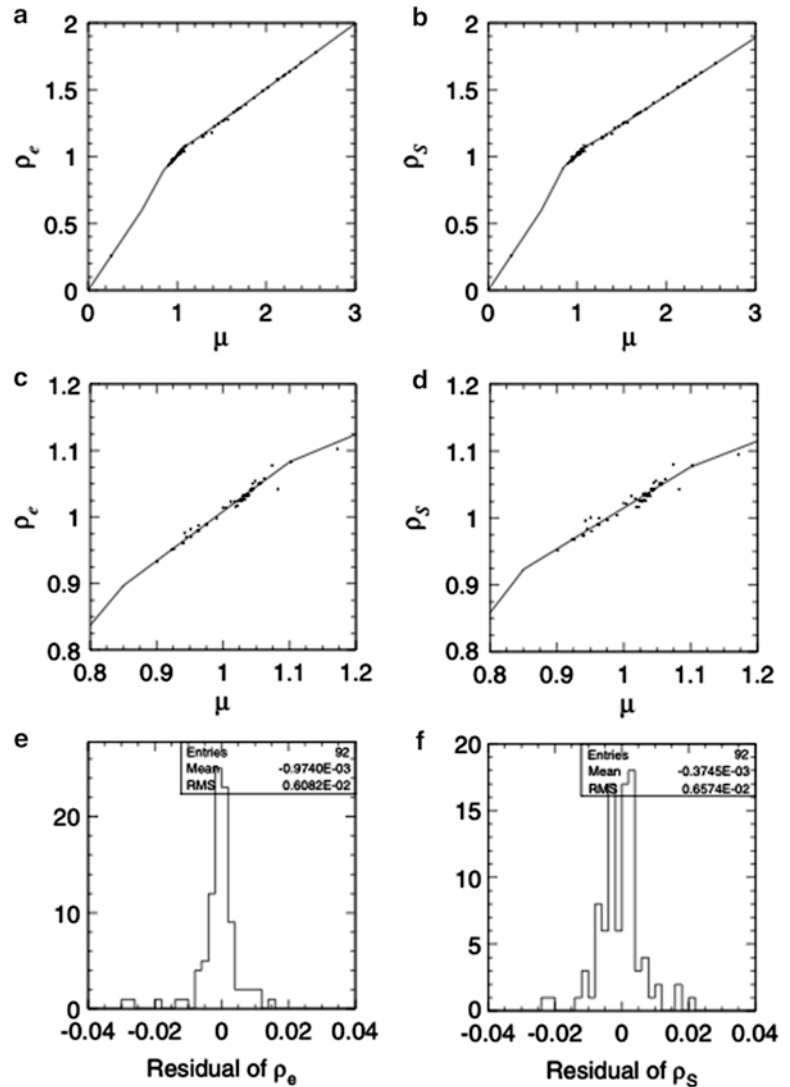
11.2.5 Plan Review

In general, common tools for treatment planning, such as isodose contours on a CT image and dose-volume histograms (DVHs), are useful also for C-ion RT, where the dose refers to the RBE-weighted dose for clinical evaluation.

For a treatment in multiple positions, one cannot simply sum individual dose distributions on different CT images using rigid image-registration techniques because the patient is usually deformed in different positions. Instead, deformable image-registration techniques may have to be used. Otherwise, for clinical dose evaluation purposes, a virtual plan is made for a virtual treatment machine that delivers equivalently oriented beams in one of the positions. The virtual plan may be useful for clinical review to assess the planned treatment of the patient.

During the review of treatment plans, uncertainties in the treatment planning and delivery process should be considered. The uncertainty in the dose distribution due to patient setup or range calculation may be assessed by calculating dose distributions for the hypothetic cases that include intentional perturbations for patient position and target depth by their estimated uncertainties. This procedure is often referred to as assessment of robustness.

In the scheme where the clinical RBE is an unambiguously formulated definition rather than estimation, no uncertainty is given to the RBE. In other words, the RBE-weighted dose is the basis of prescription as the most relevant quantity to clinical endpoints. Incidentally, the true RBE may be only derived from results of clinical studies. However, direct estimation of the RBE between carbon-ion and the reference X-ray radiations is often impossible due to differences of their standard treatment protocols in fractionation scheme.

11.3   Treatment Planning for Broad-Beam Delivery

11.3.1   Library of Standard Beams

In general, an ion beam should form a field of SOBP that covers a given target volume. In practice, the treatment planning and delivery systems have a common library of standard beams to cover a variety of possible target volumes in diameter, thickness, and depth. In the case of NIRS, there are a few energies, a few field diameters, and many different SOBP in steps of typically 1 cm. For each combination of the energy, the field diameter, and the SOBP, up to several different wobbling conditions are needed to achieve sufficiently uniform field with varied range shifter thickness for possible target depths. For each of these field-formation conditions, the beam properties such as field size, SOBP, range, and physical and clinical depth-dose curves are registered as the standard beams. There are as many as several hundred standard beams at NIRS that need to be defined and registered in the treatment planning system.

11.3.2   Field Customization

The broadened beam has to be collimated to conform to the projected target contour with an appropriate lateral margin to secure sufficiently high dose (normally 95 % of a prescribed dose) to a PTV. As the field is defined as the 50 % fluence contour, distance between 50 and 95 % may be a nominal lateral margin, which approximately coincides with the penumbra width (20–80 %).

There are several different beam-collimation devices whose setting parameters need to be determined in treatment planning. Jaw-type collimators are primarily for radiation-protection purposes and thus normally set to the minimum opening that does not affect the treatment field. A multileaf collimator is a cost- and labor-effective method for collimation. Alternatively, a patient collimator is placed close to the patient to obtain sharp lateral penumbra.

The most significant advantage of carbon-ion beams is the capability of beam-range control within the field. A range shifter is set to reduce the beam range to the maximum depth of the PTV with a depth margin that accounts for additional range uncertainty. A range compensator absorbs the excess of the beam range in the field so that the distal end of the SOBP coincides with the distal end of the PTV with the depth margin. Normally, the range compensation is designed with a simple ray-tracing calculation of the water-equivalent depth. Figure 11.3 shows the principle for range compensator design and ridge-filter selection, where w_1 and w_2 are proximal and distal water-equivalent depths of a target. The
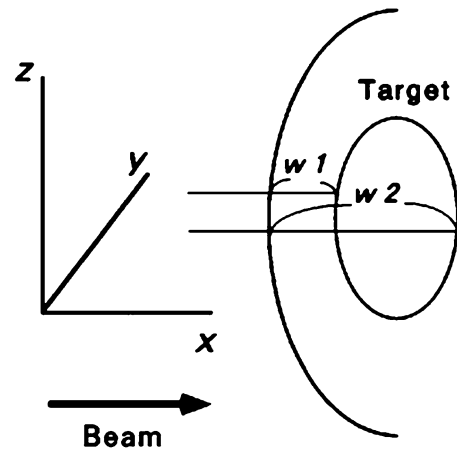

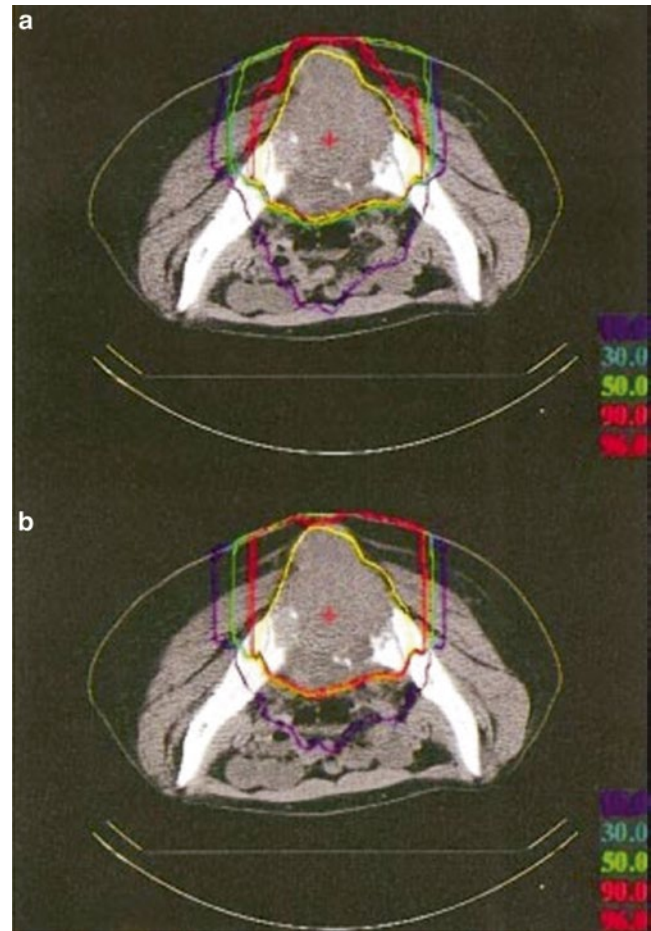**Fig. 11.3** Schematic of target analysis for range compensator design and ridge-filter selection [2]

Fig. 11.4 Dose distributions of (**a**) layer-stacking and (**b**) conventional beams for osteosarcoma in pelvis (*yellow contour*) [3]

thickness of the range compensator should be the difference to the maximum of w_2. The ridge filter should have an SOBP larger than the maximum of w_2-w_1.
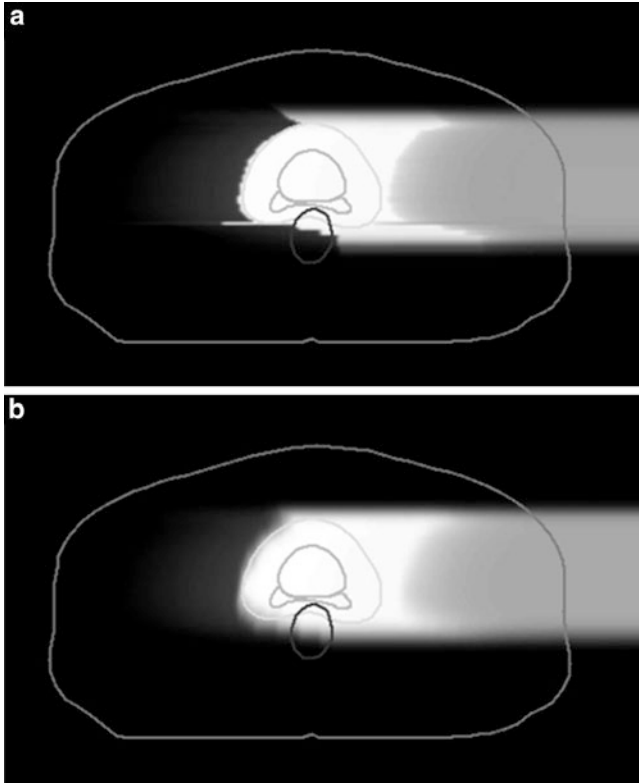
Fig. 11.5 Clinical dose distributions in grayscale from a carbon-ion beam for prostate treatment calculated with the (**a**) broad-beam and (**b**) pencil-beam algorithms [4]

In the conventional carbon-ion beam delivery, a ridge filter is used to form an SOBP to cover the PTV. However, since the SOBP has a fixed SOBP width, the SOBP in the proximal side cannot be conformal to the PTV. Therefore, the treated volume is normally conformal to the PTV by overlapping multiple fields.

In the layer-stacking delivery, a multileaf collimator field is dynamically conformed to the target in a layer-by-layer manner, which brings improved sparing to the organ at risk (OAR) proximal to the target, typically skin. Figure 11.4 shows an example of dose-distribution difference between the conventional and layer-stacking beams.

11.3.3 Dose Calculation Algorithms

Because the carbon-ion receives little scattering, the broad-beam algorithm is a reasonable approximation, in which variation of beam scattering effects are ignored and only common penumbra effects on the periphery of the field are simulated. This is simple and fast algorithm but lacks accuracy for highly heterogeneous systems. The pencil-beam algorithm models the field as comprised of two-dimensionally arranged pencil beams, which can reproduce realistic beam blurring of the field. Figure 11.5 shows an example of com-

parison between the two algorithms, where the broad-beam algorithm caused unrealistically sharp distal falloff except for the field penumbra region. Such artifacts due to algorithmic limitations must be carefully considered in dose-distribution analysis.

11.4 Treatment Planning for Scanning-Beam Delivery

In treatment planning for a passive beam delivery, the depth-dose profile is fixed by the ridge filter and no further optimization is necessary. In other words, in the system, there is no degree of freedom once a beam direction has been determined. On the other hand, the scanning-beam delivery system can produce nearly arbitrary shapes of the SOBP. To support this flexibility, two most relevant requirements on the treatment planning for the scanning system are:

- A physical beam model has to be established which describes the ion interaction with the matter, e.g., beam delivery devices and tissues, and the resultant dose distribution delivered in a patient with sufficient accuracy. Such a model should also provide the radiation quality of the beam requisite for the calculation of RBE in the patient.
- An algorithm has to be developed which is able to determine the particle number delivered to each Bragg peak position predetermined within or a small distance outside the target volume to achieve the prescribed dose distribution in the patient. This may include the optimization of the scan trajectory on each slice of equal radiological depth.

11.4.1 Beam Model

11.4.1.1 Beam Model for Calculating Absorbed Dose

In scanning-beam delivery, the prescribed dose distribution is realized by superimposing the dose of the individual pencil beams d according to their optimized weights w. The Bragg peak of the pristine beam is slightly broadened to produce a "mini peak" by the ridge filter [5]. The dose distribution at (x_i, y_i, z_i) delivered by the pencil beam stopped at (x_0, y_0, z_0) can be represented as follows:

$$d\left(x_i, y_i, z_i; x_0, y_0, z_0\right) = \\ D_1\left(x_i; x_0, y_i; y_0, \sigma_1\left(z_i; z_0\right)\right) d_z\left(z_i; z_0\right). \quad (11.1)$$

Here, $d_z(z_i; z_0)$ is the planner-integrated dose at a depth of z_i, while $D_1(x_i; x_0, y_i; y_0, \sigma_1(z_i; z_0))$ is the two-dimensional normalized Gaussian functions with standard deviations $\sigma_1(z_i; z_0)$ representing the beam spread at a depth z_i.
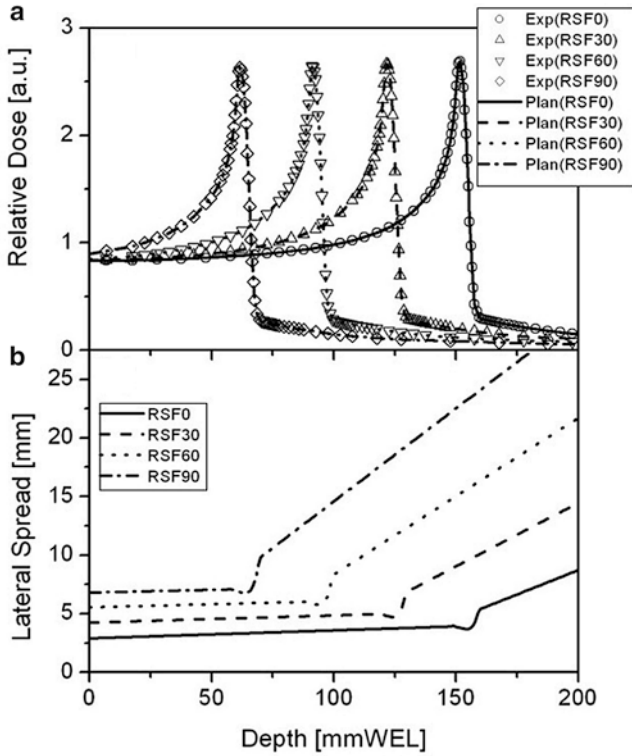
Fig. 11.6 Pencil-beam data for a 290 MeV/u carbon beam used by the treatment planning software. (**a**) Planner-integrated dose distribution d_z and (**b**) lateral beam spread σ_1 as a function of depth z_i for a range shifter of 0 (*solid line*), 30 (*dashed line*), 60 (*dotted line*), and 90 mm (*dash-dotted line*) water-equivalent thicknesses

The planner-integrated dose $d_z(z_i;z_0)$ and the lateral beam spread, i.e., $\sigma_1(z_i;z_0)$, were determined from the measured dose distribution with a large area parallel plate ionization chamber and a profile monitor, respectively. These data are fitted to simple formulae and incorporated into the planning software as shown in Fig. 11.6. With this algorithm, the effect of the beam spread due to multiple scattering in the range shifter can be incorporated, at least for the primary particles. However, our recent research revealed that the dose delivered to the target is reduced according to the field size in carbon-ion scanning with range shifter plates [6]. The observed dose reduction is referred to as the "field-size effect of dose" in this text. In order to account for this effect, we adopted three-Gaussian forms of lateral dose distributions. In this form, Eq. (11.1) can be rewritten as

$$
\begin{aligned}
d\left(x_i, y_i, z_i; x_0, y_0, z_0\right) = \\
d_z\left(z_i;t\right) \times \left\{ \left(1 - \sum_{j=2}^{3} f_j\left(z_i;t\right)\right) D_1\left(x_i;x_0, y_i;y_0, \sigma_1\left(z_i;t\right)\right) \right\}, \\
+ \sum_{j=2}^{3} \left(f_j\left(z_i;t\right) D_j\left(x_i;x_0, y_i;y_0, \sigma_j\left(z_i;t\right)\right)\right)
\end{aligned}
$$

(11.2)

where $f_j(z_i;t)$ is the fraction of integrated dose assigned to the jth Gaussian component at a depth z_i delivered by the pencil beam with the range shifter plate of thickness t, and $D_j(x_i; x_0, y_i; y_0, \sigma_j(z_i;t))$ is a two-dimensional Gaussian function describing the lateral spread of the jth component at a depth of z_i with the standard deviation $\sigma_j(z_i;t)$. The parameters $\sigma_j(z_i;t)$ and $f_j(z_i;t)$ are experimentally determined and incorporated into the planning software. The lateral dose profile expressed with the three-Gaussian beam model is schematically shown in Fig. 11.7, along with that of the single-Gaussian beam model. The observed field-size effect of doses can be accounted for with this beam model. Figure 11.8 shows comparison of the measured- and planned-absorbed dose distribution with three-Gaussian beam model for a cylindrical target of 100 mm in diameter and 60 mm in SOBP. To shorten the planning time, a dose distribution calculated with the single-Gaussian beam model is simply scaled with the factor derived with the three-Gaussian beam model to account for the field-size effect of the doses [6].

11.4.1.2 Beam Model for Calculating RBE

The absorbed dose is not sufficient to predict the biological and clinical effects of a carbon-ion beam. To make optimal use of its characteristics, the clinically relevant dose, which is defined as the product of the absorbed dose and the RBE, has to be calculated in carbon-ion treatment planning. Since various kinds of ions with various kinetic energies coexist in therapeutic carbon-ion beams, the absorbed dose and the RBE should be evaluated carefully for the accurate calculation of the clinically relevant dose. In the past decades, two different biological models have been developed to predict the RBE in mixed radiation fields of therapeutic carbon-ion beams: an empirical model developed and has been used at the National Institute of Radiological Sciences (NIRS) [7] and the local effect model (LEM) [8, 9]. These models were integrated into the treatment planning systems and successfully used in patient treatments with passive beam delivery and scanning-beam delivery at the facilities in Japan and Germany, respectively. In the treatment planning of the scanning-beam delivery, a new biological model based on the microdosimetric kinetic model (MKM) [10–12] has been developed and adopted in clinical treatments to make the maximum advantage of the scanning method as well as the excellent clinical results achieved under the current passive beam delivery. The model parameters were determined to give the best fit to the data reported by Furusawa et al. [13] for HSG tumor cells which have been used to develop the empirical model [7]. With this procedure, we could keep the continuity from the clinical experiences with the passive beam delivery.

In the MKM, the cell nucleus is divided into many microscopic sub-volumes called domain. The cell survival fraction is predicted from the energy imparted to these domains, the
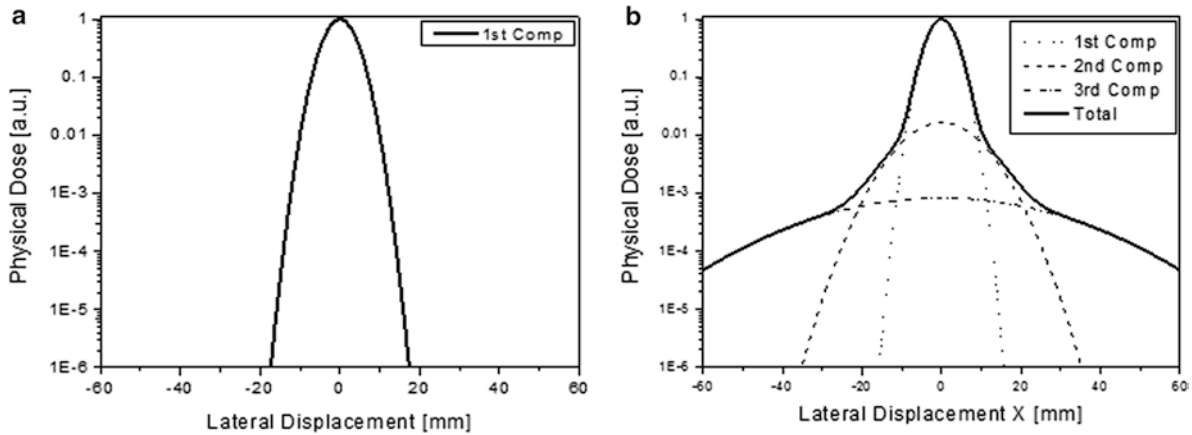
Fig. 11.7 Schematics of the lateral dose distribution expressed by (**a**) a single-Gaussian beam model and (**b**) a three-Gaussian beam model
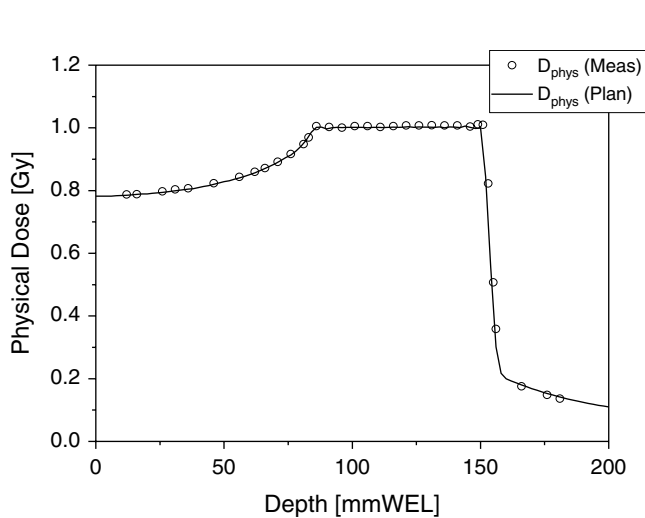

Fig. 11.8 A comparison of measured (*open circles*) and planned (a *solid curve*) absorbed dose distribution for a cylindrical target with 100 mm in diameter and 60 mm in SOBP. One Gy is prescribed to the target

Fig. 11.9 (**a**) Depth-dose and (**b**) depth-z^* distribution for a scanned carbon-ion beam with 290 MeV/u

dose mean specific energy z^*, for any kinds of radiation. To simulate the radiation quality (ion species and their kinetic energies) of the therapeutic carbon-ion beam and to predict z^* of the beam, we use the Monte Carlo code Geant4. Figure 11.9 shows the depth-dose and depth-z^* distribution for a scanned carbon-ion beam with 290 MeV/u. The mathematical procedures to calculate the RBE of therapeutic carbon-ion beam in the treatment planning system are described in detail in [15] and omitted here. To confirm the reliability of the procedures, irradiation of HSG cells was performed with a scanned carbon beam at HIMAC. In Fig. 11.10, the measured depth-survival curve is compared with the prediction based on the MKM.
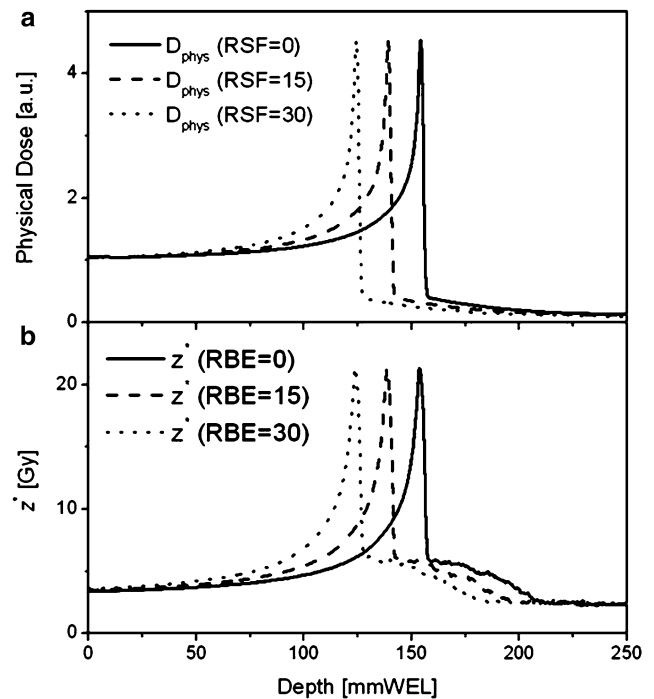
11.4.2 Dose Optimization

11.4.2.1 Optimization Algorithms

The goal of dose optimization in the treatment planning is to find the best particle numbers (weight) for each pencil beam, w, so that the resulting dose distribution is as close as possible to the prescribed dose distribution within the target volume and does not exceed the dose restrictions within the organs at risk. When determining w, the dose-based objective

function $f(w)$ is minimized through an iterative optimization process. The objective function can be described as

$$f(w) = \sum_{i \in \mathrm{T}} \left(Q_\mathrm{P}^\mathrm{o} \mathrm{H}' \left[D_{biol,i}(w) + U_i - D_\mathrm{P}^\mathrm{max} \right]_+^2 \right)$$
$$+ Q_\mathrm{P}^\mathrm{u} \mathrm{H}' \left[D_\mathrm{P}^\mathrm{min} + U_i - D_{biol,i}(w) \right]_+^2$$
$$+ \sum_{i \in \mathrm{O}} Q_\mathrm{O} \mathrm{H}' \left[D_{biol,i}(w) + U_i - D_\mathrm{O}^\mathrm{max} \right]_+^2 \quad (11.3)$$

where $D_{biol,i}(w)$, $D_\mathrm{P}^\mathrm{max}$, $D_\mathrm{P}^\mathrm{min}$, Q_P^o, Q_P^u, $D_\mathrm{O}^\mathrm{max}$, Q_O are the biological dose at a point i obtained with the matrix w, the maximum and minimum doses applied to the target T, the penalties for over- and underdosage specified for the target, the maximum

Fig. 11.10 Comparison between the measured and predicted depth-survival fraction for HSG tumor cells

dose allowed for the OAR, and the penalty for overdosage in OAR, respectively. $H'[r]$ is described as $H'[r] = rH[r]$ with the Heaviside step function, $H[r]$, defined so as to take the value of 1 only if r is greater than zero; otherwise, it takes the value of 0. In raster scanning irradiation, the beam delivery is not switched off during the transition time from one spot to the next. Therefore, in this scheme, the extra dose is inevitably delivered to the sites between two successive spots during the beam spot transition, along the scan trajectory. The contribution of the extra dose is included in the dose optimization by adding the term U_i to the objective function representing the amount of the extra dose delivered to a voxel i [6]. For the dose optimization, a number of mathematical algorithms have been proposed [14]. We used a gradient-based algorithm with the quasi-Newton method, because of its fast convergence.
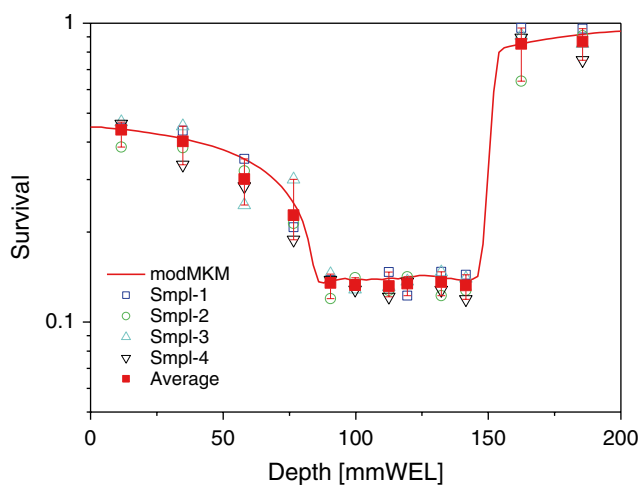
11.4.2.2 Single-Field Uniform Dose (SFUD)

The separate optimization of single treatment fields is referred to as single-field uniform dose (SFUD) optimization. To obtain a homogeneous dose, SFUD includes an intensity modulation of individual fields.

11.4.2.3 Intensity-Modulated Particle Therapy (IMPT)

In intensity-modulated particle therapy (IMPT), the nonuniform dose distributions are delivered from several directions, and the desired dose distribution is obtained after superposing the dose contributions from all fields. IMPT has the ability to deliver highly conformal dose distributions to tumors of complex shapes, while preventing the undesired exposure to neighboring OARs. Figure 11.11a shows an example of IMPT plan for a cervical chordoma patient.
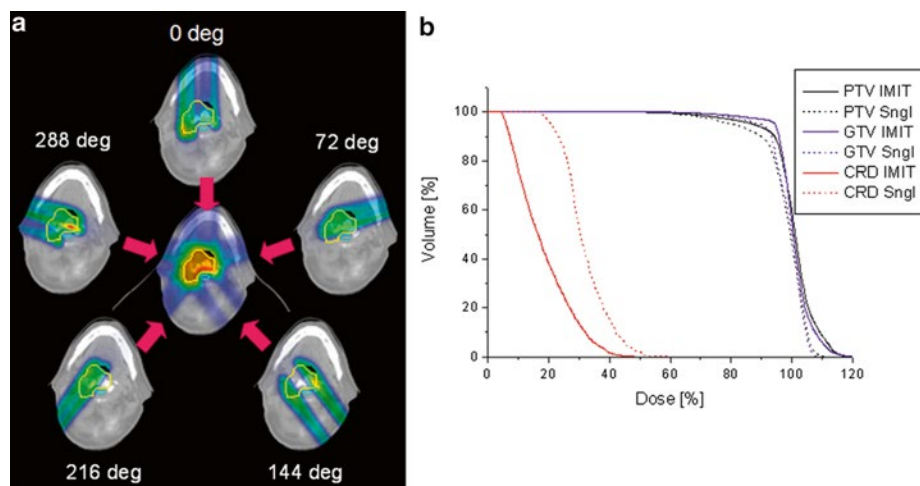

Fig. 11.11 (**a**) CT images of the cervical chordoma patient with color-wash biological dose display. The *yellow line* outlines the PTV and the *watery lines* delineate the OARs (spinal cord and brain stem). A five equidistant, coplanar beam setup was chosen during planning. (**b**) Dose-volume histogram of a five separate-beam plan (*dashed curves*) and a five-beam IMIT plan (*solid curves*) for the cervical chordoma patient

Fig. 11.12 DVHs of (**a**) reduced planning target (PTV2), (**b**) rectum (OAR), (**c**) prostate (GTV, CTV), and urethra (OAR) for a prostate treatment with carbon ion (C) or proton (p) and with broad-beam and scanning techniques
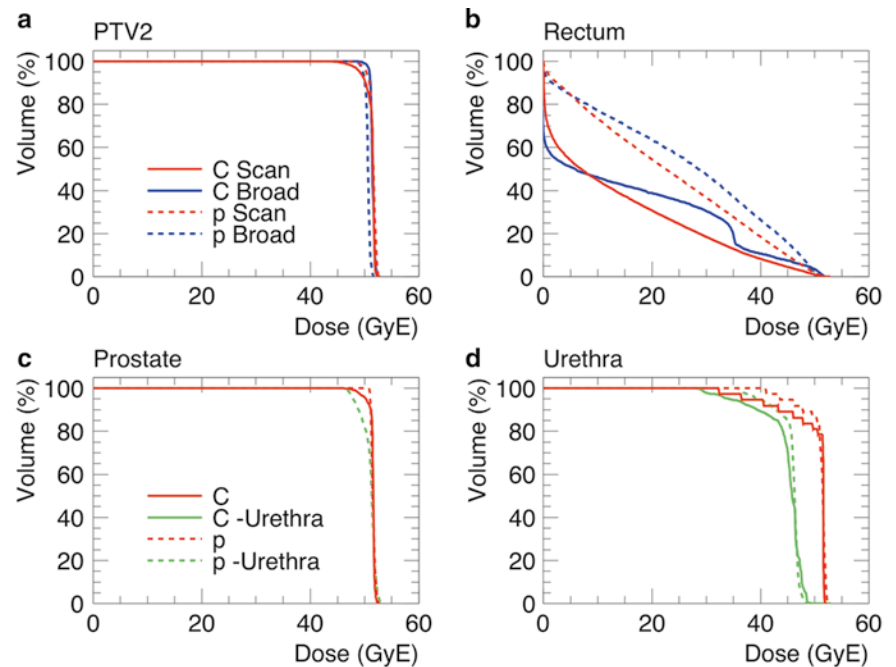
A five equidistant, coplanar beam setup was chosen for the treatment plan. Corresponding DVHs are shown with solid curves in Fig 11.11b. The dashed curves indicate the DVHs for SFUD plan with the same beam configuration. It can be seen that the dose delivered to the spinal cord could be reduced by a factor of 2.0 using the IMPT plan without any deterioration in dose conformation to the PTV as compared to the single-field plan.

11.5 Plan Comparison

Treatment planning is a dose optimization process and therefore there may be multiple plans for a treatment, one of which may be chosen for prescription. In such decisions, among many aspects to be considered, the dose distribution is the most essential information. Especially the curative dose coverage for the PTV and dose control below tolerance level for OAR are in most cases objectively evaluated with DVHs. However, as the PTV involves peripheral margin regions, which may be often compromised to spare OARs, DVH for various PTVs, CTVs, and GTV may possibly give supplemental information for plan evaluation.

For example, Fig. 11.12 compares DVHs for a prostate treatment planned with proton and carbon-ion beams with the broad-beam and scanning delivery techniques. For scanning-beam plans, optimization with and without urethra sparing were tested. In this case, the proton beams suffered from increased rectum dose due to larger lateral penumbra.

The urethra-sparing optimization in fact resulted in reduced urethra dose for the scanning beams.

References

1. Kanematsu N, Matsufuji N, Kohno R, Minohara S, Kanai T. A CT calibration method based on the polybinary tissue model for radiotherapy treatment planning. Phys Med Biol. 2003;48:1023–64.
2. Endo M, Koyama-Ito H, Minohara S, Miyahara N, Tomura H, Kanai T, Kawachi K, Tsujii H, Morita K. HIPLAN–a heavy ion treatment planning system at HIMAC. J Jpn Soc Ther Radiol Oncol. 1996;8:231–8.
3. Kanematsu N, Endo M, Futami Y, Kanai T, Asakura H, Oka H, Yusa K. Treatment planning for the layer-stacking irradiation system for three-dimensional conformal heavy-ion radiotherapy. Med Phys. 2002;29:2823–9.
4. Kanematsu N, Yonai S, Ishizaki A. Grid-dose-spreading algorithm for dose distribution calculation in heavy charged particle radiotherapy. Med Phys. 2007;35:602–7.
5. Weber U, Kraft G. Design and construction of a ripple filter for a smoothed depth dose distribution in conformal particle therapy. Phys Med Biol. 1999;44:2765–75.
6. Inaniwa T, Furukawa T, Nagano A, Sato S, Saotome N, Noda K, Kanai T. Field-size effect of physical doses in carbon-ion scanning using range shifter plates. Med Phys. 2009;36:2889–97.
7. Kanai T, Endo M, Minohara S, Miyahara N, Koyama-Ito H, Tomura H, Matsufuji N, Futami Y, Fukumura A, Hiraoka T, Furusawa Y, Ando K, Suzuki M, Soga F, Kawachi K. Biophysical characteristics of HIMAC clinical irradiation system for heavy-ion radiation therapy. Int J Radiat Oncol Biol Phys. 1999;44:201–10.
8. Scholz M, Kraft G. Track structure and the calculation of biological effects of heavy ion beams for therapy. Adv Space Res. 1996;18:5–14.
9. Elsässer T, Weyrather WK, Friedrich T, Durante M, Iancu G, Krämer M, Kragl G, Brons S, Winter M, Weber KJ, Scholz M.

Quantification of the relative biological effectiveness for ion beam radiotherapy: direct experimental comparison of proton and carbon ion beams and a novel approach for treatment planning. Int J Radiat Oncol Biol Phys. 2010;78:1177–83.

10. Hawkins RB. A statistical theory of cell killing by radiation of varying linear energy transfer. Radiat Res. 1994;140:366–74.

11. Kase Y, Kanai T, Matsumoto Y, Furusawa Y, Okamoto H, Asaba T, Sakama M, Shinoda H. Microdosimetric measurements and estimation of human cell survival for heavy-ion beams. Radiat Res. 2006;166:629–38.

12. Inaniwa T, Furukawa T, Kase Y, Matsufuji N, Toshito T, Matsumoto Y, Furusawa Y, Noda K. Treatment planning for a scanned carbon ion beam with a modified microdosimetric kinetic model. Phys Med Biol. 2010;55:6721–37.

13. Furusawa Y, Fukutsu K, Aoki M, Itsukaichi H, Eguchi-Kasai K, Ohara H, Yatagai F, Kanai T, Ando K. Inactivation of aerobic and hypoxic cells from three different cell lines by accelerated ^{3}He-, ^{12}C- and ^{20}Ne-ion beams. Radiat Res. 2000;154:485–96.

14. Nocedal J, Wright SJ. Numerical optimization (Springer series in operations research). New York: Springer; 1996.